MOLECULAR AND CELLULAR BIOLOGY, July 1988, p. 2848–2859
0270-7306/88/072848-12$02.00/0

Vol. 8, No. 7

TRK1 Encodes a Plasma Membrane Protein Required for High-Affinity Potassium Transport in *Saccharomyces cerevisiae*

RICHARD F. GABER,[1]* CORA A. STYLES,[2] AND GERALD R. FINK[2]

Northwestern University, Evanston, Illinois 60208,[1] and Whitehead Institute for Biomedical Research, Cambridge, Massachusetts 02167[2]

Received 4 February 1988/Accepted 14 April 1988

We identified a 180-kilodalton plasma membrane protein in *Saccharomyces cerevisiae* required for high-affinity transport (uptake) of potassium. The gene that encodes this putative potassium transporter (*TRK1*) was cloned by its ability to relieve the potassium transport defect in *trk1* cells. *TRK1* encodes a protein 1,235 amino acids long that contains 12 potential membrane-spanning domains. Our results demonstrate the physical and functional independence of the yeast potassium and proton transport systems. *TRK1* is nonessential in *S. cerevisiae* and maps to a locus unlinked to *PMA1*, the gene that encodes the plasma membrane ATPase. Haploid cells that contain a null allele of *TRK1* (*trk1*Δ) rely on a low-affinity transporter for potassium uptake and, under certain conditions, exhibit energy-dependent loss of potassium, directly exposing the activity of a transporter responsible for the efflux of this ion.

Various different proteins appear to mediate the transport of potassium across cell membranes. In higher eucaryotes, the well-characterized Na^+/K^+-ATPase and a number of K^+ channels mediate functionally distinct mechanisms for K^+ transport. The mammalian Na^+/K^+-ATPase has been purified and reconstituted in vitro (7), and the DNA sequences of cDNAs that encode the α and β subunits of this enzyme have been determined (14, 33, 34). The only K^+ channel for which the amino acid sequence has been inferred is that encoded by the *Shaker* gene in *Drosophila melanogaster* (13, 23, 36). Little if any homology exists between the subunits of the Na^+/K^+-ATPase and this K^+ channel. The differences between these two avenues of K^+ transport are also reflected in their functional aspects. Whereas the Na^+/K^+-ATPase couples the pumping of K^+ ions directly to ATP hydrolysis, K^+ channels mediate the transport of this ion essentially by diffusion through an ion-specific pore independent of ATP hydrolysis.

The bacterial K^+-translocating ATPase encoded by the *kdpABC* genes (6) shares a number of features with the mammalian Na^+/K^+-ATPase. Both are multisubunit enzymes that depend directly on ATP hydrolysis for K^+ transport. In addition, they share regions of amino acid homology (9, 34). In contrast, K^+ uptake in *Neurospora crassa* can occur by transport that is directly coupled to the symport of protons (26). K^+ transport is driven in this case by the energy inherent in a large proton gradient across the plasma membrane generated by the plasma membrane H^+-ATPase. Thus, the *Neurospora* K^+ and H^+ symporter is only indirectly dependent on ATP hydrolysis. Structural aspects of this K^+ transporter remain unknown.

K^+ transport across the plasma membrane of *Saccharomyces cerevisiae* results in a 1,000-fold concentration gradient of this ion. Although yeast cells grow on medium containing as little as 5 μM potassium (27), intracellular K^+ levels reach approximately 150 mM (2). Recent reports have identified some of the proteins that may be responsible for the generation and maintenance of the potassium gradient. Yeast cells contain a plasma membrane H^+-ATPase (30), at least one species of K^+ channel (8), and a transport system that mediates the uptake of potassium with multiple affinities (27). The relationship between these transporters remains to be determined, but the evidence suggests that they represent functionally independent molecules. Purified and reconstituted H^+-ATPase mediates proton translocation and ATP-ADP exchange in vitro in the absence of potassium (18, 19). The identification of *TRK1*, a gene required for high-affinity K^+ uptake in *S. cerevisiae* (25), has made possible genetic experiments that demonstrate that the H^+-ATPase and *TRK1* are encoded by unlinked loci (this report).

The recent report of the cloning of the plasma membrane ATPase gene (*PMA1*) by Serrano et al. (31) has set the stage for a molecular genetic analysis of K^+ transport. We are attempting to unravel the components of K^+ transport in *S. cerevisiae* through the use of mutations that block transport and by isolation of the genes defined by those mutations. We initiated our investigation with experiments designed to (i) distinguish between direct and indirect coupling of K^+ and H^+ transport and (ii) determine whether the dual-affinity system for K^+ uptake described by Rodriguez-Navarro and Ramos (27) consists of a single transporter or multiple, functionally independent transporters.

In this report, we identify yeast genes involved in potassium transport. Only mutations at *TRK1* confer a significant defect in high-affinity transport of this ion, although mutations in several other genes lead to an increased requirement for extracellular potassium. Our results show that high-affinity K^+ uptake occurs via an independent transporter functionally distinct from both the plasma membrane H^+ pump and low-affinity K^+ uptake activity. The data suggest that *TRK1* is the structural gene for the high-affinity potassium transporter.

MATERIALS AND METHODS

Media, strains, and plasmid constructions. YPD and YNB media and routine genetic techniques are described by Sherman et al. (32). LS medium, containing less than 2 μM sodium and virtually no potassium before addition, was made essentially as described by Ramos et al. (25), with the exception that ammonia was substituted in the place of arginine as the nitrogen source. Yeast transformation was performed by the LiAc method of Ito et al. (12). The strains

* Corresponding author.

TABLE 1. Strains used in this study

Species and strain	Genotype[a]	Reference or source
E. coli HB101	*hsdS20 recA13 ara-14 proA2 lacY1 galK2 rpsL20 xyl-15 mtl-14 supE44*	20
S. cerevisiae		
R757	α *his4-15 ura3-52 lys9*	This study
R1030	α *ura3-52 lys9 trk1-1*	This study
R1154[b]	α *his4-15 ura3-52 lys9 trk1Δ::URA3:: TRK1*	This study
R1155	α *his4-15 ura3-52 lys9 trk1Δ*	This study
R1168[c]	α *ura3-52 lys9 trk1-1::URA3*	This study
R676	**a** *his4-15 ura3-52*	This study
R1193	α *his4-15 ura3-52 lys9*(pRG296-1)	This study
R1205	α *his4-15 ura3-52 lys9*(pGN621)	This study
R1206	α *his4-15 ura3-52 lys9 trk1Δ*(pGN621)	This study
4753-6D[c]	**a** *ura3-52 ino1 cdc6 trk1-1::URA3*	This study
4754-10A	α *ura3-52 ura2 leu2-3 leu2-112*	This study
PC1	α *ade2-1 adeX trk1-1*	25
L1937	**a** *his4-713 ura3-52*	T. Donahue

[a] For descriptions of plasmids within yeast strains, see Materials and Methods.

[b] Strain R1154 contains plasmid pRG319-2 integrated at the *TRK1* locus.

[c] Strains R1168 and 4753-6D contain plasmid pRG277-1 integrated at the *trk1-1* locus.

and plasmids used are described in Table 1. Plasmids were selected and propagated in *Escherichia coli* HB101 (20).

Yeast strain R1155, containing a deletion within the *TRK1* gene, was generated by the method of integration and excision (39). Plasmid pRG319-2, containing *trk1Δ*, was constructed by first subcloning the 10-kilobase (kb) *Sal*I-*Pvu*II fragment carrying *TRK1* into *Sal*I- and *Eco*RI-digested YIp5 in which the *Eco*RI site was blunt ended with the *E. coli* polymerase I large fragment (Klenow). The *TRK1*-internal 2.35-kb *Xba*I fragment was then removed by digestion with *Xba*I and subsequent recircularization by ligation. Yeast strain R1154, containing the *trk1Δ URA3 TRK1* duplication, was constructed by transformation of strain R757 to a Ura+ phenotype with plasmid pRG319-2. Cells having lost the plasmid sequences through mitotic recombination were selected as Ura− segregants of strain R1154 that were resistant to 5-fluoro-orotic acid (1). Plasmid pRG296-2, containing yeast 2μm sequences and *TRK1*, was constructed by subcloning the 9.5-kb *Sal*I-*Eco*RI fragment from pRG272-1 into plasmid pGN621 (a gift of Georges Natsoulis). pGN621 is YIp5 with yeast 2μm sequences inserted at the *Sma*I site near *URA3*.

Plasmid pRG378-1, containing the *trpE::TRK1* gene fusion, was constructed by subcloning the 652-base-pair *Msp*I-*Sal*I fragment encompassing the 3′ end of *TRK1* from plasmid pRG295-1 into *Cla*I and *Sal*I-digested plasmid pATH2 (a gift of A. Tzagoloff). The resulting gene fusion encodes a hybrid protein containing the C-terminal 103 amino acids of Trk1.

Genetic mapping. Standard linkage values were derived from tetrad data by using the equation X (in centimorgans) = 50[tetratype asci + 6(nonparental ditype asci)]/total asci (24). Gene order in multipoint crosses was determined by analyzing recombinant asci containing crossovers in the regions of interest.

Isolation of potassium-dependent mutants. Mutants that require the higher concentrations of potassium in the medium for growth were selected by using a method described by Ramos et al. (25). The method takes advantage of the difference in resistance to heat between wild-type cells and mutants. Mutant cells, when preincubated in a nonpermissive medium, are more resistant to a short heat treatment than are wild-type cells (38). The nonpermissive medium was K^+-limiting medium containing 1 mM KCl (LSK1) that lacked added potassium. Medium containing 100 mM KCl was chosen as the permissive medium to avoid the isolation of osmotic sensitive mutants that may require significantly higher concentrations of potassium. Independent cultures of strain R757 (Table 1) were mutagenized with ethyl methanesulfonate and grown in YPD medium supplemented with 100 mM KCl (YPD100K). After growth in liquid YPD100K, the cells were incubated at 30°C for 4 h in LS medium and then subjected to 54°C for 6 min. The heat-treated cultures were allowed to grow inYPD100K to permit growth of mutants among the survivors. After this growth, the cultures were again starved for potassium in LS medium and subjected to a second round of heat treatment. Survivors were plated on YPDK100 solid medium. The resulting colonies were replica plated to LS agar medium containing 1 mM (LSK1) and 100 mM (LSK100) KCl and then incubated at 30°C. Potassium-dependent mutants (Kdm^-) were identified as colonies that grew normally on LSK100 but showed no growth or decreased growth on LSK1.

Fractionation of yeast cells. Fractionation of yeast cells into soluble, mitochondrial, microsomal, and plasma membrane fractions was derived from the method of Malpartida and Serrano (18, 19). One-liter cultures of yeast cells were grown to a density of 4×10^7 cells per ml in YNB supplemented with all amino acids and 100 mM KCl (but lacking uracil) containing 2% glucose. The cells were harvested and washed twice in 25 ml of double-distilled H_2O and suspended in 2 ml of buffer A (100 mM Tris hydrochloride, 10 mM EDTA, 2 mM phenylmethylsulfonyl fluoride, 2 μg of Pepstatin [pH 8.0] per ml). Phenylmethylsulfonyl fluoride and Pepstatin were obtained from Sigma Chemical Co. Two milliliters of cell suspension was placed in a 35-ml polyallomer tube to which 10 ml of cold glass beads was added. All subsequent steps were carried out in the cold. The cells were broken by vortexing and then diluted with 20 ml of buffer B (20% glycerol, 10 mM Tris, 1 mM EDTA, 0.1 mM dithiothreitol [pH 7.5]). The resulting homogenate was separated into a crude pellet and a supernatant (3K supernatant) by centrifugation at 3,000 rpm for 10 min. The mitochondrial and plasma membrane fractions were pelleted by centrifugation of the 3K supernatant at 16,000 rpm for 20 min. Microsomes were removed from the 16K supernatant by pelleting at 40,000 rpm for 1 h, and the soluble fraction was retained as the 40K supernatant. The mitochondrial-plasma membrane pellet was homogenized in a Dounce homogenizer with the type B pestle in 2 ml of buffer B, and 1 ml of the homogenate was layered onto a sucrose step gradient (0.35 ml of 53% sucrose in solution B and 0.7 ml of 43% sucrose in solution B) and run in a Beckman SW55 rotor at 55,000 rpm for 30 min. The mitochondria accumulated in an upper band, and the plasma membranes accumulated in a lower band. The plasma membranes were collected with an 18-gauge needle and a 1-ml syringe, diluted three or four times in double-distilled H_2O, and pelleted with 35,000 rpm for 15 min. The purified plasma membranes were then suspended in Laemmli buffer (16) before polyacrylamide gel electrophoresis.

Polyclonal antiserum to glycerol-3-phosphate dehydrogenase and a monoclonal antibody to cytochrome oxidase subunit III were generously provided by Tom Mason. Alkaline phosphatase-coupled secondary antibody to mouse im-

munoglobulin (Promega Biotech) was used to detect binding of these primary antibodies to filter-bound proteins.

Plasma membrane ATPase assays. Assay of yeast plasma membrane ATPase was performed as described by Serrano (29).

Protein determinations. Total protein from *S. cerevisiae* was obtained by trichloroacetic acid extraction as previously described (22). Protein concentrations of total yeast extracts or membrane fractions were determined by the method of Lowry (17). Bovine immunoglobulin G was used as the protein standard.

DNA manipulations. Rapid plasmid DNA isolation was done by the method of Holmes and Quigley (11); restriction analysis, gel electrophoresis, and Southern analysis were as described by Maniatis et al. (20). Hybridization probes were made as described by Maniatis et al. (20). The *TRK1*-specific probe was prepared by gel purification of the 2.35-kb *Xba*I fragment that had been subcloned into pBR322. Filters containing the hybridized probe were washed either four times in 0.1× SSC (1× SSC is 0.15 M NaCl plus 0.015 M sodium citrate)–0.1% sodium dodecyl sulfate (SDS) at 65°C (high stringency) or four times in 6× SSC–0.1% SDS at 55°C (low stringency) before autoradiography.

DNA sequence analysis of the *TRK1* gene. DNA sequence analysis of both strands of the 4.2-kb *Sal*I-*Bam*HI fragment was accomplished by the method of Sanger et al. (28). Random DNA fragments generated by sonication (21), as well as subcloning of specific restriction fragments into M13 vectors, facilitated the analysis.

High-affinity potassium uptake assay. The ability of yeast cells to mediate high-affinity uptake of potassium was measured as follows. Cells were grown to a density of 6×10^7/ml in YNB supplemented with 100 mM KCl but lacking uracil to maintain selection for plasmids. The cells were harvested, washed with double-distilled H_2O, and starved for 3 to 4 h at a density of 1.8×10^8 in 50 mM Tris-succinate (pH 5.9) on an orbital shaker at 30°C. Starved cells were harvested by centrifugation, washed in double-distilled H_2O, suspended at a density of 6×10^9 cells per ml, and kept on ice. A 0.5-ml volume of the cell suspension was taken for each uptake assay and diluted to a final volume of 5 ml in a medium made to 50 mM Tris-succinate–1 mM KCl–2% glucose (pH 5.9). The glucose was added last, and the concentration of potassium in the medium was monitored with a potassium-specific electrode (Orion 931900) with constant agitation of the cell suspension. Typically, high-affinity uptake assays were performed over a period of 10 to 15 min at 21°C.

Insertional mutagenesis. Introduction of frameshift mutations into the *TRK1* gene was accomplished by insertion of CGGATCCG *Bam*HI linkers (Collaborative Research, Inc.) into the *Alu*I, *Hae*III, and *Rsa*I sites of plasmid pRG295-1. After partial digestion by one of these restriction endonucleases and dephosphorylation with calf intestinal phosphatase (Miles Laboratories, Inc.), linear-size molecules were gel purified and ligated with a 50-fold molar excess of phosphorylated *Bam*HI linkers. Plasmids containing linker insertions were isolated by transformation of *E. coli* HB101 to ampicillin resistance. Plasmid DNA was prepared from these transformants, and the relative locations of the linker insertions were determined by mapping the novel *Bam*HI site.

Construction of *trpE::TRK1* gene fusion. An in-frame gene fusion was made between the *E. coli trpE* gene and *TRK1* by joining the *Hpa*II site at +3395 (Asp 1133) in *TRK1* and the *Cla*I site at the carboxy-terminal end of *trpE* in the vector pATH2 (a gift of A. Tzagoloff). The resulting plasmid (pRG378-1) encoded a hybrid protein containing the carboxy-terminal 103 amino acids of Trk1 fused to the carboxy-terminal end of the TrpE protein (see Fig. 10). Induction of the *trpE* operon and subsequent purification of a novel 47.5-kilodalton (kDa) hybrid protein were performed as described by Spindler et al. (35).

Preparation of antiserum. Approximately 20 μg of gel-purified TrpE-Trk1 hybrid protein was emulsified in Freund complete adjuvant and injected intraperitoneally into rabbits. A similar injection in Freund incomplete adjuvant was given as a boost after 4 and 6 weeks. Antiserum was collected 1 week later. Yeast proteins were separated by SDS-polyacrylamide gel electrophoresis and transferred electrophoretically to nitrocellulose sheets (37). The nitrocellulose sheets were incubated with the antiserum, and antibodies bound to filters were detected by incubation with ^{125}I-labeled goat anti-rabbit antibody (New England Nuclear Corp.).

RESULTS

Potassium-dependent mutants. We isolated 239 mutants that require elevated levels of extracellular potassium for normal growth. Isolation of K^+-dependent mutants was performed as described in Materials and Methods. Approximately 10% of the survivors of the heat selection enrichment scheme exhibited decreased growth on minimal levels of potassium (1 mM; LSK1) compared with growth on higher levels of the ion (100 mM; LSK100). Subsequent tests demonstrated that 10 mM potassium was sufficient to allow maximal growth of all mutants isolated from this selection. Each mutant was crossed with strain L1937, and the resulting Kdm^-/Kdm^+ diploids were tested for their Kdm phenotypes on LSK1. Growth of the diploids on this medium was indistinguishable from that of R757/L1937 (Kdm^+/Kdm^+) diploids, demonstrating that each of the mutations isolated was recessive.

One Kdm^-/Kdm^+ heterozygous diploid was sporulated, and tetrads dissected from this cross showed a 2:2 segregation pattern for the Kdm^-/Kdm^+ phenotypes. This mutant was designated *kdm1-1*, and a representative *kdm1-1 MAT***a** recombinant was picked for complementation tests of the remaining 238 Kdm^- mutants. Of the 239 mutants obtained from 23 independent cell lines, 153 were allelic to *kdm1-1*. Genetic analysis performed on the remaining 86 Kdm^- mutants revealed seven additional complementation groups. *kdm2* contained 72 mutants, *kdm3* contained one mutant, *kdm4* contained four mutants, *kdm5* contained five mutants, and a single mutant in each of the *kdm6*, *kdm7*, and *kdm8* complementation groups was obtained.

Six independent *kdm1* alleles were tested by complementation and recombination with the potassium-dependent *trk1-1* strain isolated by Ramos et al. (25). None of our *kdm1* mutants complement the *trk1-1* mutant strain. Furthermore, tetrad analysis of spores dissected from sporulated *kdm1/trk1-1* diploids indicated comlete genetic linkage between these mutations (data not shown). These tests show that the *kdm1* complementation group is allelic to *trk1*. In keeping with the nomenclature established by Ramos et al. (25), our independent alleles of this gene are designated *trk1-11* through *trk1-16*.

Representatives of each *kdm* complementation group were crossed with the Kdm^+ strain L1937, and the resulting diploids were sporulated for dissection of tetrads. Tetrad analyses of each of these crosses showed a 2:2 segregation for the Kdm^- and Kdm^+ phenotypes, with the exception of

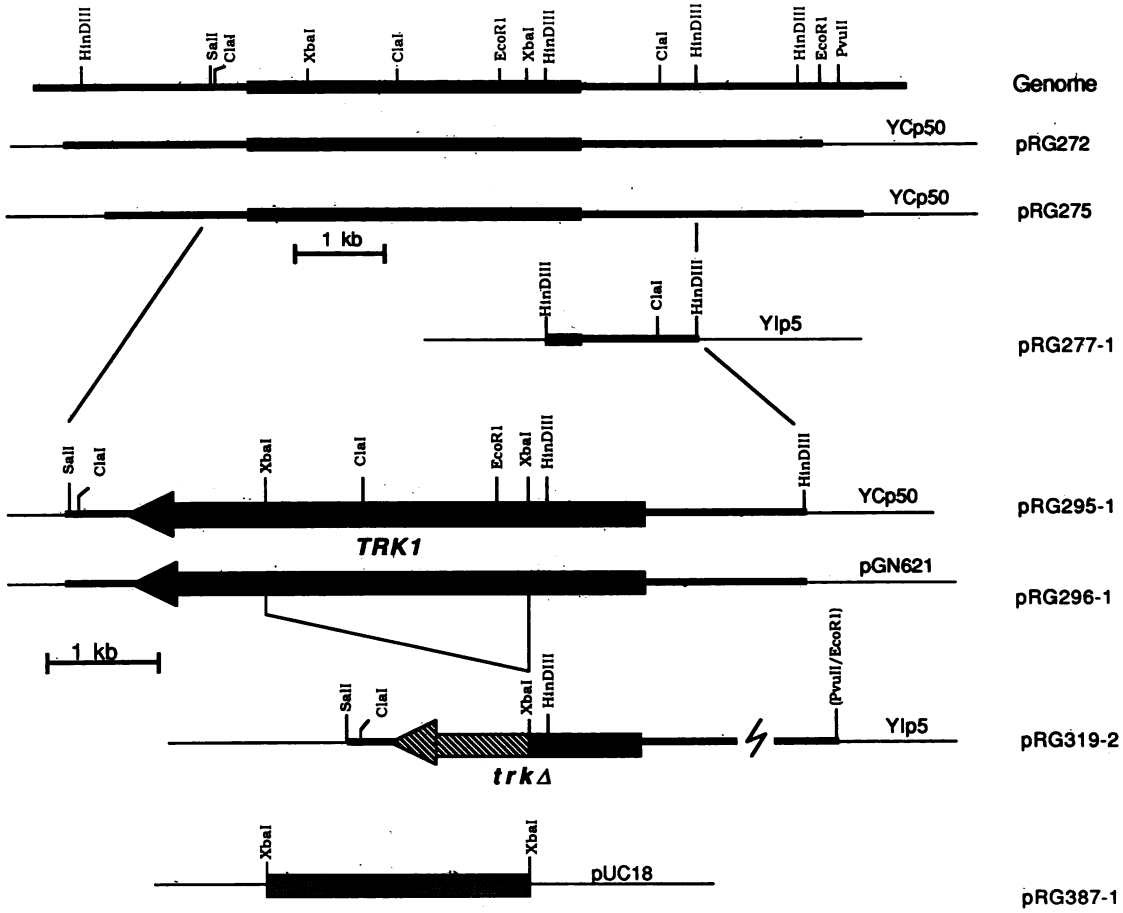

FIG. 1. Restriction endonuclease sites of the yeast *TRK1* gene and construction of a deletion mutation within the *TRK1* gene. Genomic clones (pRG272 and pRG275) are described in Results and Materials and Methods. Subclones (pRG277-1, pRG295-1, pRG296-1, pRG319-2, and pRG387-1) were constructed as described in Materials and Methods. The shaded arrows in pRG295-1 and pRG319-2 represents the inframe protion of *TRK1*; the striped arrow in pRG319-2 represents the out-of-frame portion generated by deletion of the internal *Xba*I fragment.

kdm6. The excess of Kdm^+ spores from the *kdm6* × L1937 cross suggested that the potassium-dependent phenotype of *kdm6* depends upon the presence of more than one mutation.

A growth requirement dependent on high extracellular K^+ could result from a number of different defects. To identify K^+ transport-defective mutants, we screened the *kdm* mutants for their ability to take up potassium. The assays measured the rate and extent of K^+ depletion from a buffered medium containing K^+- and glucose-starved cells (Materials and Methods). Representative mutants from each of the eight *kdm* complementation groups were specifically assayed for their ability to take up K^+ with high affinity. Only mutations in the *KDM1* (*TRK1*) group were defective in high-affinity uptake; the reamining *kdm2* through *kdm8* mutants exhibited rates of K^+ uptake indistinguishable from that of wild-type cells (see Fig. 9). Because of the alteration in high-affinity K^+ uptake and because strains that carry *trk1-1* have an altered K_m for high-affinity potassium uptake (25), our initial efforts focused on the *TRK1* gene.

Isolation of the *TRK1* gene. The *TRK1* gene was cloned on the basis of its ability to suppress the potassium transport defect in *trk1* cells. The *TRK1* gene was isolated from a yeast genomic library contstructed in the shuttle vector YCp50 (a gift of Mark Rose). Plasmids pRG272-1 and pRG275-1 (Fig. 1) suppressed the increased potassium dependency of *trk1-1* strain R1030 (Table 1). *trk1-1* cells require 5 to 10 mM potassium in the medium to support maximal growth, whereas *trk1-1* transformants harboring plasmid pRG272-1 or pRG275-1 exhibit the wild-type requirement of less than 1 mM extracellular potassium. Both pRG272-1 and pRG275-1 were isolated in *E. coli* and, after retransformation into *S. cerevisiae*, were able to confer the Ura^+ Trk^+ phenotype to strain R1030.

Restriction endonuclease digests of pRG272-1 and pRG 275-1 revealed that these plasmids share a large region of overlap (Fig. 1). We performed a directed-integration experiment to determine whether the cloned DNA fragments encoded the *TRK1* gene. A 2.9-kb *Hin*dIII fragment from within the overlap region was subcloned from pRG275-1 into the integrative vector YIp5, resulting in the recombinant plasmid pRG277-1 (Fig. 1). pRG277-1 was linearized by partial digestion with *Eco*RI to direct integration to the chromosomal site homologous to the subcloned DNA fragment. Strain R1030 was transformed to a Ura^+ phenotype with this DNA, and all transformants were found to retain the parental Trk^- phenotype, suggesting that the plasmid DNA contained, at most, only part of the *TRK1* gene. One of the Ura^+ Trk^- transformants (R1168) was crossed with

TRK1 strain R676 and, after sporulation of the resulting diploid, tetrads were dissected onto permissive medium (>10 mM KCl). Tetrad analysis demonstrated complete genetic linkage between the integrated Ura^+ plasmid sequences and the Trk^- phenotype (32PD:0T:0NPD). Integration of the plasmid at the *trk1* locus confirmed that the cloned DNA fragments in plasmids pRG272-1 and pRG275-1 carry the *TRK1* gene.

A restriction map of plasmid pRG295-1 containing the cloned *TRK1* gene was generated by using a number of restriction endonucleases that recognize hexamer sequences (Fig. 1). These restriction sites were then used to construct subclones that facilitated further analysis of *TRK1*.

Genetic mapping of *TRK1*. The chromosomal location of the *TRK1* locus was determined through hybridization of a DNA fragment that encodes part of the *TRK1* gene to electrophoretically separated yeast chromosomes (3, 4). Hybridization of the 2.2-kb *Cla*I fragment purified from plasmid pRG286-1 to yeast chromosomes immobilized on filters resulted in detection of a single band corresponding to chromosome X in each of two strains that were known to exhibit different mobilities for this chromosome (data not shown). The unique signal was identified after stringent washing of the hybridized blot, suggesting that the *TRK1* gene is present in a single copy per haploid genome. Further experiments confirmed this interpretation (described below).

A more precise location of the *TRK1* locus was determined genetically by crossing strain R1168, which contains plasmid pRG277-1 integrated at the *trk1-1* locus (*trk1-1::URA3*, described above) with strains that carry different chromosome X markers. Genetic linkage was detected between *trk1-1::URA3* and the markers *ino1*, *cdc6*, and *ura2*. A four-point mapping cross was generated by crossing strains R4753-6D and R4754-10A (Table 1). Tetrad analysis of the meiotic progeny obtained from this cross is presented in Fig. 2.

Insertional mutagenesis of *TRK1*. The approximate size of the *TRK1* gene and its location within the cloned yeast DNA fragment in plasmid pRG295-1 was determined by insertional mutagenesis (Fig. 3). Frameshift mutations were introduced

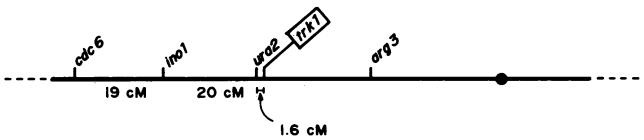

FIG. 2. Genetic map of left arm of chromosome X. The genetic distance between *trk1* and linked markers on the left arm of chromosome X is indicated in centimorgans (cM). The genetic map positions are derived in part from tetrad analysis of meiotic progeny from a cross between R4753-6D and R4754-10A (Table 1). Among 93 four-spored tetrads, 3 were tetratype with respect to the *trk1-1::URA3* and *ura2* markers. Two of these tetrads were tetratype with respect to the *trk1-1::URA3 ino1* marker pair but parental ditype for the *ura2 ino1* marker pair. The remaining *trk1-1::URA3 ura2* tetratype ascus was also tetratype for the *ura2 ino1* marker pair, parental ditype for the *ino1 cdc6* marker pair, and nonparental ditype for the *trk1-1::URA3 ino1* marker pair. These results are consistent with the order *cdc6 ino1 ura2 TRK1 arg6 CENX*. A total of three tetratype asci for the *trk1-1::URA3 ura2* marker pair out of a total of 93 tetrads gave a distance of 1.6 cM between these markers. A second cross was performed between strain 4758-10B, containing an independent *trk1-11* mutation, and strain 4757-16B (Table 1). Tetrad analysis of 103 four-spored asci obtained from this cross supported the same gene order of chromosome X markers (unpublished data).

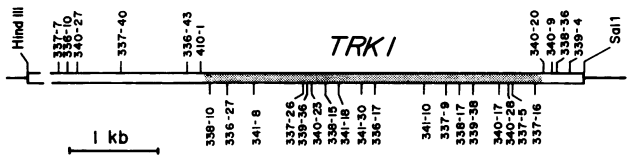

FIG. 3. Linker insertion mutations in the cloned *TRK1* gene. The numbered sites represent positions of 8-mer oligonucleotides (*Bam*HI linkers) inserted a native *Alu*I (336 and 337 series), *Hae*III (338 and 339 series) and *Rsa*I (340 and 341 series) restriction sites in plasmid pRG295-1. Linker insertions above the line had no discernable effect on function of the plasmid-borne *TRK1* gene. Linker insertions below the line destroyed the ability to complement the *trk1-1* mutation in recipient cells. The hatched region marks the approximate region defined by the *TRK1* gene.

by inserting DNA octamers that encode *Bam*HI restriction sites (linkers) into the *Alu*I, *Hae*III, and *Rsa*I sites of the cloned DNA fragment. The effect of each mutation was measured by testing for the ability of a plasmid carrying a particular *Bam*HI linker to complement the potassium uptake deficiency in the recipient *trk1* yeast strain R1030. The results of the insertion mutagenesis are summarized in Fig. 3. Linker insertions that disrupt the function of the cloned *TRK1* gene define a contiguous region of DNA over 3.6 kb long. Since the insertions represent frameshift mutations, those linkers that disrupt the function of *TRK1* were considered likely to reside within the coding region of the gene. On the basis of these results, the 4.2-kb DNA fragment extending from the *Sal*I site to the *Bam*HI site at linker 336-43 was presumed to encompass the functional *TRK1* gene (Fig. 3).

DNA sequence analysis of *TRK1* gene. The nucleotide sequence of the *TRK1* gene was determined by DNA sequence analysis of the 4.2-kb *Sal*I-*Bam*HI fragment contained in a pRG295-1 derivative that carried *Bam*HI linker 336-43 (Fig. 3). A single open reading frame of 3,705 base pairs was found 21 nucleotides downstream from a noncanonical TATA box (Fig. 4). The first ATG sequence of this open reading frame is located 180 nucleotides downstream from the *Bam*HI linker insertion 336-43. The location of the open reading frame corresponds to that predicted by the insertional-mutagenesis experiments. Each of the *Bam*HI linker insertions that disrupted the function of *TRK1* maps within the open reading frame of the gene.

The predicted amino acid sequence determined from the *TRK1* open reading frame encodes a protein of 1,235 amino acids with a molecular mass of 141 kDa. The 40 N-terminal amino acids make up a largely hydrophilic domain and thus do not appear to constitute a signal sequence for vectorial insertion across membranes. The AsnAsnAsnAsnAsnAsn AsnArgLysLysLysLysLysLysLys sequence at position 1,044 to 1,058 and the AspMetAspAspAspAspAspAspAsp AspAsnAspGlyAsp sequence at position 1,500 to 1,545 generate two highly charged domains within the protein. A computer-assisted comparison of the predicted Trk1 protein sequence and amino acid sequences in the available data banks failed to find any matches of extensive identity. However, several small but significant regions of amino acid identity should be mentioned. Short stretches of identical sequences were found between Trk1 and the acetylcholine receptor α subunit of *Torpedo californica* and between Trk1 and the *E. coli* potassium-transporting ATPase encoded by the *kdpC* gene (Fig. 5). In the acetylcholine receptor α subunit, 7 amino acids within a stretch of 20 are identical and several represent conservative substitutions. The seven identical amino acids include a rare tryptophan and two

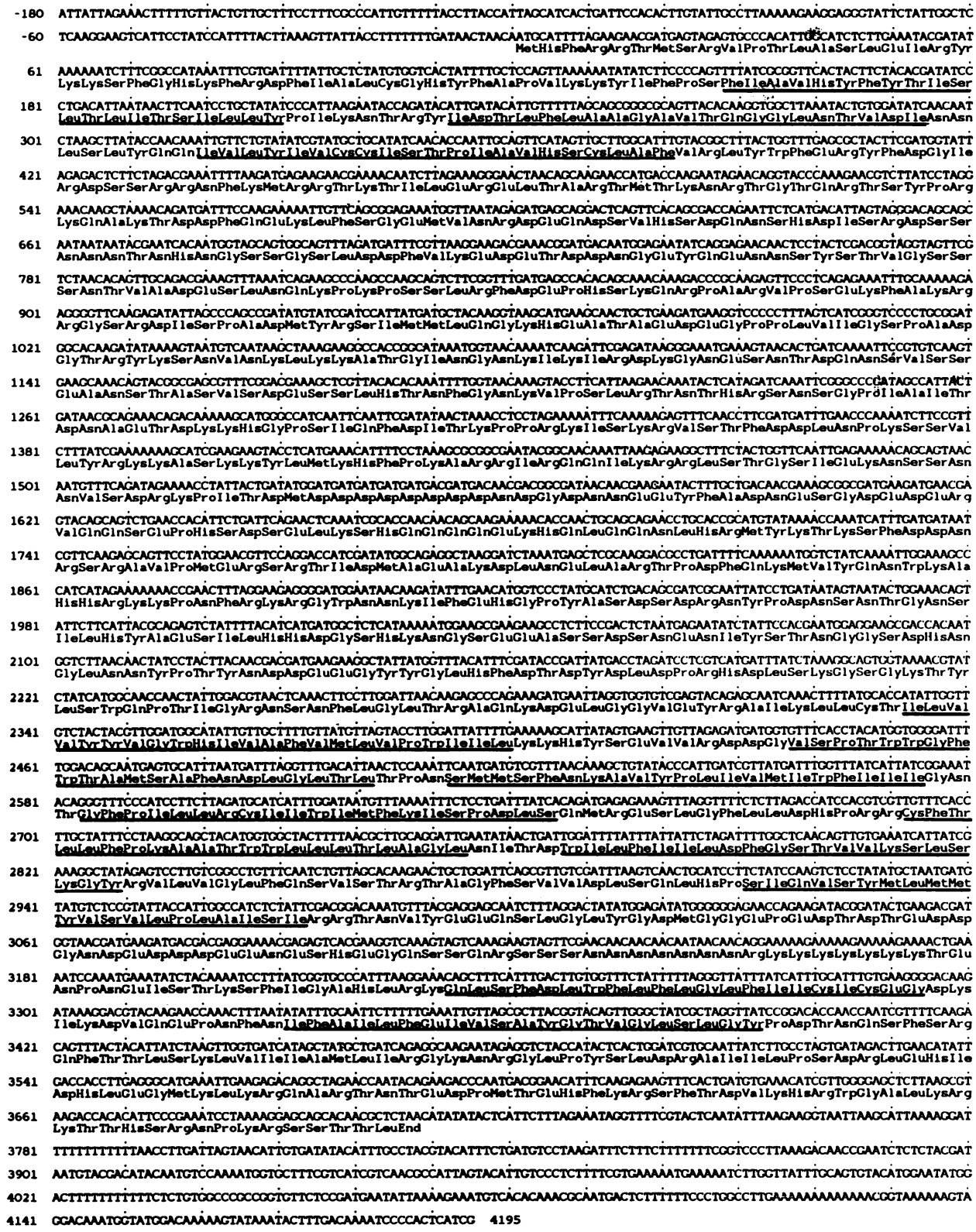

FIG. 4. DNA sequence of the *TRK1* gene. The DNA sequence of the region from the *Bam*HI linker site 336-43 to the *Sal*I site in plasmid pRG295-1 was determined as described in Materials and Methods. A 3,705-base-pair open reading frame was identified from the sequence data. Potential membrane-spanning domains (see Results) are underlined.

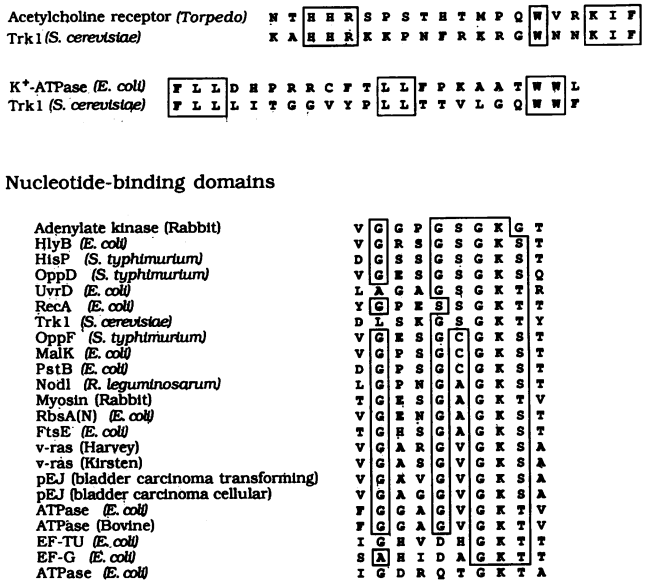

FIG. 5. Sequence identities between the predicted Trk1 protein and other proteins. The *Torpedo* acetylcholine receptor sequence is from M. Noda, H. Takahashi, T. Tanabe, M. Toyasato, Y. Furutani, T. Hiroshi, M. Asai, S. Inayama, T. Miyata, and S. Numa, Nature (London) **299**:793–797, 1982. The *E. coli* K^+-ATPase sequence and the nucleotide-binding domain sequences are from references 9 and 10, respectively.

adjacent histidine residues. In the *E. coli* K^+-ATPase, 7 amino acids within a stretch of 22 were found to be identical, with an additional 6 amino acids representing conservative substitutions. The presence of a conserved pair of adjacent tryptophans and the fact that both proteins are involved in cation transport make these limited homologies particularly intriguing.

Significant amino acid sequence identity between Trk1 and the nucleotide-binding domains of a number of procaryotic and eucaryotic proteins was also observed (Fig. 5). The sequence Gly-Ser-Gly-Lys-Thr present at position 735 to 739 in Trk1 shares four and sometimes five amino acids in common with other nucleotide-binding proteins. Conspicuously absent, however, is the glycine residue at a position three amino acids upstream, representing the first element in the conserved nucleotide-binding domain. Although this glycine is strongly conserved in the Gly-Xxx-Xxx-Gly-Xxx-Gly-Lys-Thr (or Ser) sequence, at least two other nucleotide-binding proteins, UvrD and Ef-G, also differ at this position (10). The serine-to-glycine change in the last position of the core domain in rabbit adenylate kinase indicates that at least one more element of this consensus can undergo divergence.

The predicted amino acid sequence of the *TRK1* gene was used to generate a hydropathy plot as a guide to the identification of possible membrane-spanning domains within the protein. A Kyte-Doolittle (15) hydropathy plot (Fig. 6) identified a large number of hydrophobic segments encoded by *TRK1*. With the algorithm of Eisenberg (5), 12 potential membrane-spanning domains within the protein sequence encoded by *TRK1* were revealed. Based on these criteria, a preliminary structural model of Trk1 is presented

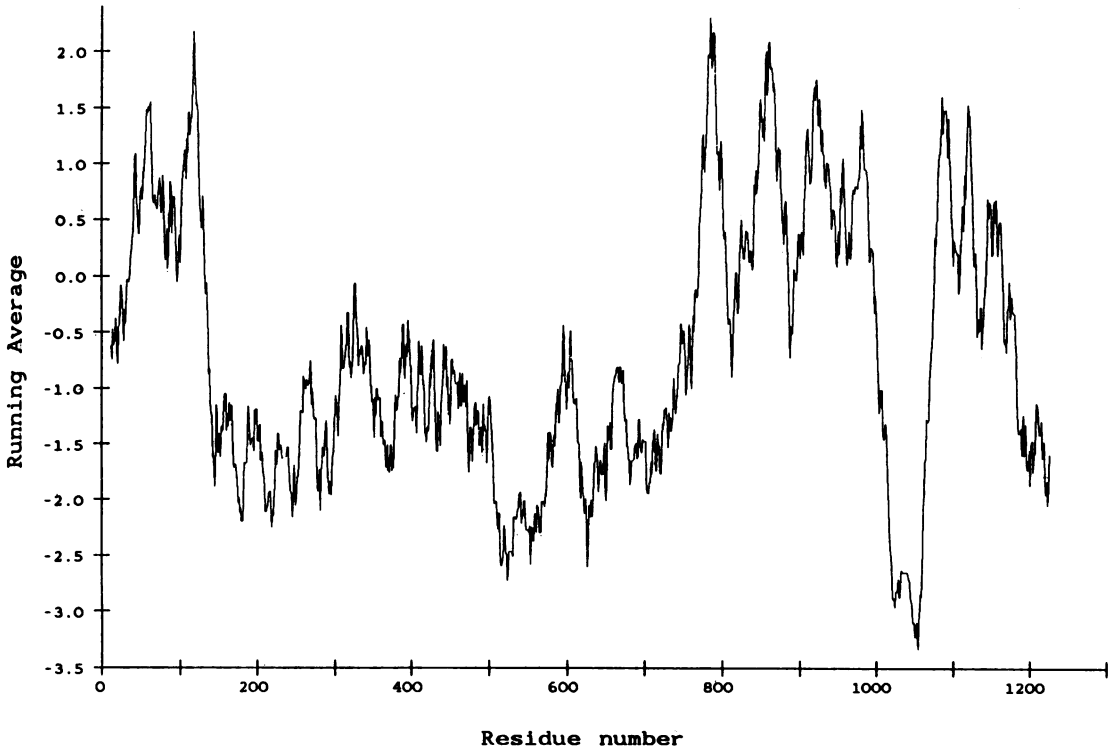

FIG. 6. Hydropathy plot of predicted Trk1 protein. Hydropathy values (15) for a window of 22 amino acid residues were averaged, assigned to the middle residue of the span, and plotted with respect to position along the amino acid sequence. The numbers refer to potential membrane-spanning domains predicted by the algorithm of Eisenberg et al. (5).

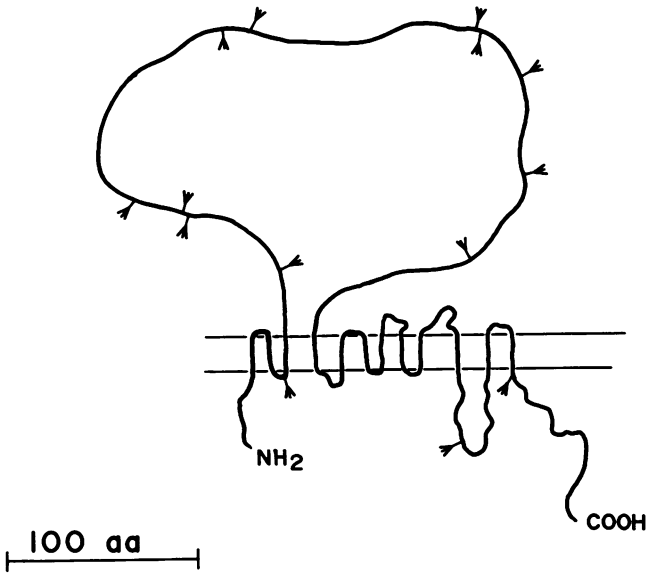

FIG 7. Model of possible orientation of predicted Trk1 protein within the yeast plasma membrane. Forked figures represent locations of N-linked potential glycosylation sites. Intracellular-extracellular orientation is unknown. aa, Amino acids.

in Fig. 7. A 650-amino-acid hydrophilic domain lies between putative membrane-spanning domains 3 and 4. Although this domain contains 12 of 15 potential N-linked glycosylation sites encoded by *TRK1*, we have no experimental evidence to indicate whether this domain is extracellular or intracellular. The short regions of identity to the acetylcholine receptor and the bacterial K^+-ATPase and the putative nucleotide-binding site correspond to regions in other proteins that are thought to reside within the cytoplasm. These regions reside within the 650-amino-acid hydrophilic region, suggesting that it represents a cytoplasmic domain.

Deletion of *TRK1* gene. Physiological results that suggest a dual system for potassium uptake in *S. cerevisiae* (27) can be explained by a single potassium transporter that has the inherent ability to change its affinity for the ion or by two functionally independent transporters with distinct K_ms. To help distinguish between these possibilities, we constructed a strain that contained a null allele of *TRK1*. Deletion of the 2.35-kb *Xba*I fragment from the coding region of the cloned *TRK1* gene was constructed in vitro (Materials and Methods), and the resulting plasmid was used to construct a *trk1*Δ *URA3 TRK1* duplication by integrative transformation of strain R757. Ura^- segregants resulting from loss of the plasmid and one of the duplicated *TRK1* regions were obtained by selection for resistance to the uracil analog 5-fluoro-orotic acid (1). Isogenic strains containing either the *trk1*Δ or *TRK1* gene were obtained by picking mitotic Ura^- Trk^- and Ura^- Trk^+ segregants, respectively. Southern analysis confirmed that the Trk^- segregants carry the deletion. The 2.35-kb *Xba*I fragment from the *TRK1* gene was purified from plasmid pRG387-1 (Fig. 2) and used to probe Southern blots of digested genomic DNA from the Trk^+ and Trk^- segregants described above. The autoradiogram shown in Fig. 8 demonstrates that the Trk^- segregant R1155 contains a deletion of the 2.35-kb *Xba*I fragment.

The fact that a haploid strain that contains the deletion is viable demonstrates that, although *TRK1* is required for high-affinity potassium uptake, it is not an essential gene in *S. cerevisiae*. This result, combined with the independent

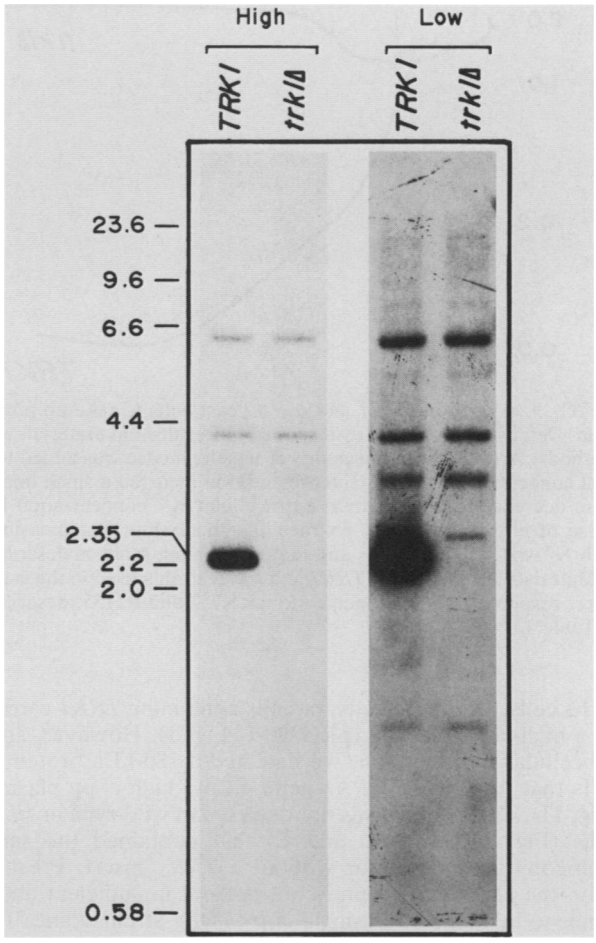

FIG. 8. Southern blot analysis of *TRK1* and *trk1*Δ genomic DNA. DNA from TRK1 and *trk1*Δ strains R757 and R1155, respectively, was digested with *Xba*I before electrophoresis and blotting to the filter. The 2.35-kb *Xba*I fragment from plasmid pRG387-1 was used as a probe and contains sequences entirely within the *TRK1* gene. High and low refer to the stringencies of the washes used to remove the ^{32}P-labeled probe and are detailed in Materials and Methods.

genetic locations of *TRK1* and *PMA1*, strongly suggests that in yeast cells high-affinity uptake of potassium and proton extrusion occur through independent transport systems.

The effect of the *trk1* deletion on potassium transport was measured in the potassium uptake assay described in Materials and Methods. Isogenic strains R757 (*TRK1*) and R1155 (*trk1*Δ) were assayed and compared for their relative abilities to mediate high-affinity potassium uptake (Fig. 9). *TRK1* cells took up over 90% of the available potassium within 10 min, whereas *trk1*Δ cells were deficient in uptake and, under the assay conditions used, actually showed a net efflux of potassium from the cell. Assays performed without addition of glucose or with addition of 2-deoxyglucose resulted in absence of detectable uptake or efflux of potassium from either strain.

Identification of *TRK1*-encoded 180-kDa membrane protein. Western blot immunoblot analysis of total yeast proteins was performed by using antiserum raised against a *trpE*::*TRK1*-encoded fusion protein (Fig. 10) as a probe (see Materials and Methods). We were unable to detect a *TRK1*-specific protein among unfractionated yeast proteins isolated from

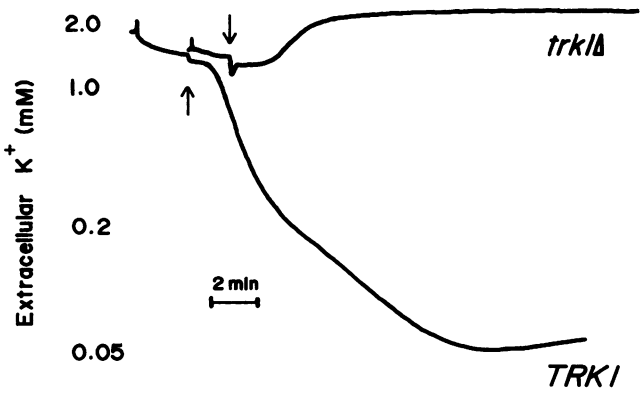

FIG. 9. Ability of *TRK1* and *trk1*Δ yeast cells to take up potassium. Details of the assay are described in Results and Materials and Methods. Arrows represent points at which glucose was added to a final concentration of 4%. Glucose addition incurred a small immediate decrease in the apparent extracellular K^+ concentration because of physical dilution. Extracellular potassium was measured with K^+-specific electrodes and plotted on a log scale as described in Materials and Methods. *TRK1* and *trk1*Δ strains used in the assay were, respectively, the isogenic strains R757 and R1155, described in Table 1.

*trk1*Δ cells, wild-type cells, or cells containing *TRK1* carried on a high-copy plasmid (pRG296-1; Fig. 1). However, after subcellular fractionation, we detected a 180-kDa protein in cells that carried the *TRK1* gene on the high-copy plasmid (Fig. 11). This protein was not detected in wild-type or *trk1*Δ cells (Fig. 11, lanes D and E) that contained the same high-copy cloning vector without a *TRK1* insert. Presumably, the 180-kDa protein is not present in sufficient abundance to be detected in single-copy *TRK1* strains (lane 5) or in crude extracts from high-copy strains (lane 2) with our current antiserum.

Subcellular localization of the Trk1 protein was examined by fractionating cells into cytoplasmic (soluble protein), mitochondrial, and plasma membrane fractions. Plasma membrane and mitochondrial fractions were isolated as described by Malpartida and Serrano (18, 19). Western blot analysis of each of the subcellular fractions demonstrated that the 180-kDa protein is localized to the plasma membrane and mitochondrial fractions (Fig. 11). A band of approximately 80 kDa, detected only in the plasma membrane fraction from R757(pRG296-1), is apparently a degradation product of Trk1, since the size and abundance of this band varied significantly in different preparations. The bands of lower molecular mass (<50kDa) detected in the total pro-

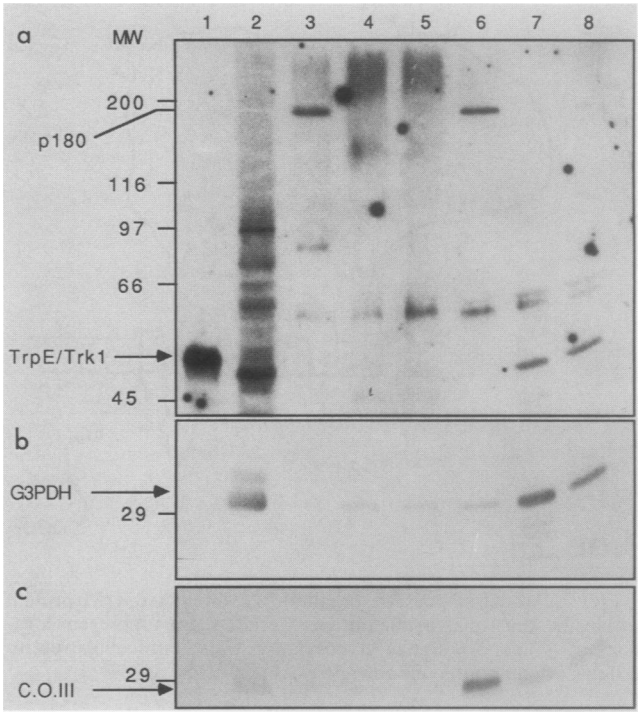

FIG. 11. Subcellular localization of Trk1 protein. Western blot analysis of subcellular fractions from wild-type strain R757 containing either the high-copy 2μm::*TRK1* plasmid pRG296-1 (lanes 2, 3, 6, 7, and 8) or the 2μm vector pGN621 without the *TRK1* insert (lane 5) and from the *trk1*Δ strain R1155 containing pGN621 (lane 4). Lanes: 1, TrpE-Trk1 fusion protein (80 ng); 2, unfractionated protein from R757(pRG296-1) (40 μg); 3, plasma membrane fraction from R757(pRG296-1) (60 μg); 4, plasma membrane fraction from R1155(pGN621) (60 μg); 5, plasma membrane fraction from R757 (pGN621) (40 μg); 6, mitochondrial fraction from R757(pRG296-1) (40 μg); 7, soluble protein from R757(pRG296-1) (40 μg); 8, microsomal fraction from R757(pRG296-1) (40 μg). The three panels outlined are from the same filter blot. (a) Trk1 protein and TrpE-Trk1 fusion protein detected with ^{125}I-labeled secondary antibody (autoradiogram exposed for 10 days). (b) Glyceraldehyde-3-phosphate dehydrogenase (G3PDH) detected with ^{125}I-labeled secondary antibody (autoradiogram exposed for 6 h). (c) Cytochrome oxidase III (C.O.III) detected with alkaline phosphatase-labeled secondary antibody. The numbers on the left indicate molecular weight (mw) in thousands.

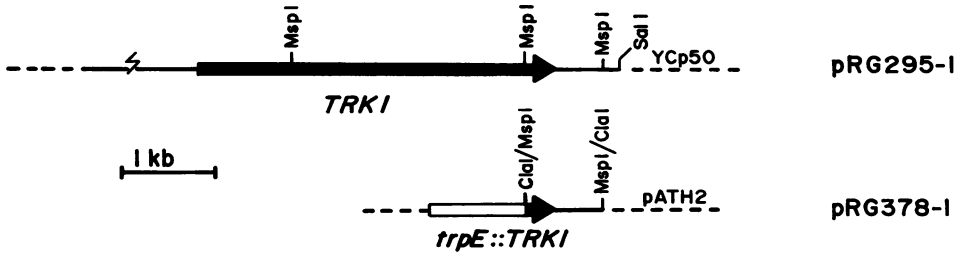

FIG. 10. Construction of *trpE*::*TRK1* gene fusion. A segment of the *TRK1* gene corresponding to the carboxy-terminal 103 amino acids of the predicted protein were spliced in frame to *trpE* carried on the pATH11 expression vector (a gift of A. Tzagoloff) as described in Materials and Methods. Hybrid TrpE-Trk1 protein was made in *E. coli* HB101 from the *trpE*::*TRK1* gene fusion carried on plasmid pRG378-1 as described in Materials and Methods.

tein, soluble fraction,and microsomal fraction were present in equivalent amounts in *TRK1* high-copy, wild-type, and *trk1*Δ strains (data not shown). The identity of these proteins is not known.

As controls, the subcellular fractions were also probed with antibodies to glyceraldehyde-3-phosphate dehydrogenase (Fig. 11b) and cytochrome oxidase subunit II (Fig. 11c). Glyceraldehyde-3-phosphate dehydrogenase was observed primarily in the soluble and microsomal fractions, as well as in the unfractionated protein, with only small quantities in the plasma membrane fraction. Cytochrome oxidase subunit II was detected in significant amounts only in the unfractionated protein and mitochondrial fraction.

Plasma membrane ATPase assays performed on each of the fractions revealed significant ATPase activity in the plasma membrane and the mitochondrial fractions (0.43 and 0.24 milliunits/mg of protein, respectively) but not in the soluble and microsomal fractions. The results indicate that, with the exception of significant plasma membrane contamination of the mitochondrial fraction, the fractionation procedures are relatively specific for their respective subcellular components. Repeated homogenization and sucrose density centrifugation did not appreciably reduce the level of plasma membrane contamination in the mitochondrial fraction. Although we cannot rule out the possibility that Trk1 is localized to the mitochondria as well as the plasma membrane in vivo, detection of Trk1 in the mitochondrial fraction may be due to plasma membrane contamination.

The apparent size of the Trk1 protein is approximately 40 kDa larger than that predicted by the sequence of *TRK1*. This discrepancy may represent aberrant mobility on SDS gels because of a number of highly charged domains it contains or, possibly, because of glycosylation of the transporter at any of the 14 potential N-linked glycosylation sites in the molecule. However, treatment of the plasma membrane fraction with endoglycosidase H failed to decrease the apparent molecular weight of Trk1 on SDS gels (data not shown).

DISCUSSION

We cloned the *TRK1* gene and showed that it is required for high-affinity potassium transport (uptake) in *S. cerevisiae*. Although we did not rule out the possiblity that *TRK1* is a positive regulator of the high-affinity uptake system, several lines of evidence suggest that *TRK1* is the structural gene that encodes the high-affinity transporter. (i) among a large number of mutants isolated, only mutations in *TRK1* result in defective uptake of potassium. (ii) The results of a molecular analysis of the *TRK1* gene indicate that it encodes an integral membrane protein. The 1,235-amino-acid protein predicted from the DNA sequence contains 12 hydrophobic regions 20 to 22 amino acids long that are potential membrane-spanning domains on the basis of the algorithm of Eisenberg (5). Antibodies raised against the *TRK1* gene product detect a 180-kDa protein that is localized to the yeast plasma membrane, consistent with its role in K^+ transport. Two regions within the 650-amino-acid hydrophilic domain of the predicted protein share small but significant homologies with other cation-transporting proteins: the acetylcholine receptor in *T. californica* and the K^+-translocating ATPase in *E. coli*. Ramos et al. (25) have shown that the *trk1-1* allele confers an altered K_m for potassium. Taken together with this evidence, our data support the contention that the high-affinity potassium transporter of *S. cerevisiae* is encoded by *TRK1*.

The possibility that Trk1 functions as a K^+-translocating ATPase is suggested by the presence of a putative nucleotide-binding domain within the protein. On the other hand, nucleotides may play only a regulatory role and Trk1 might facilitate passive transport by acting as a K^+ channel. Because our experiments did not discriminate between active and passive transport, we use the general term transporter in describing Trk1.

We isolated mutations in eight complementation groups, each of which confers a potassium-dependent phenotype. Only mutations in *TRK1* resulted in a significant decrease in the ability to take up potassium from the medium. The potassium transport assay we used as a screen measured net uptake of potassium from the medium into cells when the extracellular concentration of the ion was low (1 mM). Although the screen was designed to identify mutants defective for high-affinity uptake of potassium, it is possible that any or all of the remaining mutant groups, *kdm2* through *kdm8*, represent defects in some other component of the potassium transport system of the cell but failed to show a defect in our assay. Alternatively, these mutants may take up potassium normally but require higher intracellular concentrations of potassium for growth.

Our results suggest that a dual-affinity potassium transport system in *S. cerevisiae* consists of two functionally independent transporters. The description by Ramos et al. (25) of a mutant (*trk1-1*) defective in high-affinity uptake but normal for low-affinity uptake implied that two distinct proteins are responsible for potassium transport. However, this study was unable to distinguish between a single transporter with dual affinity and multiple potassium transporters, because the nature of the *trk1-1* mutation, and therefore its effect on the activity of Trk1 protein, was not known. To address this question, we created a *trk1* null allele by constructing a haploid strain with a large internal deletion in the gene. Since deletion of *TRK1* from haploid cells leaves the low-affinity system intact, *TRK1* cannot be responsible for both high- and low-affinity uptake. Yeast cells must have an additional, functionally independent potassium transporter of lower affinity.

Our mutant screen precluded the isolation of mutations in the low-affinity transporter. Rodriguez-Navarro and Ramos (27) demonstrated that low-affinity K^+ uptake exhibits a K_m of approximately 2 mM. The existence of a functionally independent high-affinity transporter may have masked the phenotype of any mutants in the independent low-affinity transporter. In further support of this hypothesis, we have recently isolated mutations that affect the low-affinity potassium transporter, and their analysis is in progress.

Our experiments demonstrate that *trk1*Δ cells lack the ability to take up potassium when extracellular concentrations are low (below 1 mM) and actually exhibit energy-dependent efflux of potassium under these conditions. Although potassium efflux occurs in wild-type cells as well (2), it is masked under the conditions of our assay by the activity of *TRK1*. The net K^+ efflux observed from *trk1*Δ cells is likely to represent the inability of these cells to recapture escaping potassium when the extracellular concentration of this ion is sufficiently low. Thus, a null allele of *TRK1* completely disrupts high-affinity potassium uptake in *S. cerevisiae* and, under certain conditions, permits direct observation of the function of an independent transporter responsible for efflux of this ion. It is possible that both low-affinity uptake and the observed efflux may represent a reversal of K^+ flux through a single transporter. The observed efflux of K^+ could be coupled to the influx of H^+ in

an electroneutral exchange, or it may represent actual K^+ extrusion resulting in hyperpolarization of the membrane. Since both low-affinity uptake and efflux of K^+ have become amenable to genetic analysis through deletion of *TRK1*, such possibilities can be adressed through further mutational studies.

Our data demonstrate the functional and physical independence of the K^+ and H^+ transport systems in *S. cerevisiae*. Genetic analysis revealed that the *TRK1* locus is located approximately 1.6 centimorgans (centromere proximal) from the *URA2* gene on chromosome X. Since *TRK1* is unlinked to *PMA1*, the gene that encodes the plasma membrane ATPase, the putative K^+ transporter, and the H^+ pump are encoded by distinct genes. This result supports the hypothesis that proton extrusion and high-affinity potassium uptake in *S. cerevisiae* are only indirectly coupled, a result further supported by the nonessential nature of *TRK1*.

ACKNOWLEDGMENTS

We thank A. Rodriguez-Navarro for supplying us with the PC1 strain, Jan Peters and Laura Best for excellent technical assistance, and Marc Vidal for critical reading of the manuscript.

This work was supported by Public Health Service postdoctoral fellowship 5F32GM09383-03 (to R.F.G.) from the National Institutes of Health.

LITERATURE CITED

1. **Boeke, J. D., F. Lacroute, and G. R. Fink.** 1984. A positive selection for mutants lacking orotidine-5'-phosphate decarboxylase activity in yeast: 5-fluoro-orotic acid resistance. Mol. Gen. Gene. **197**:345–346.
2. **Borst-Pauwels, G.** 1981. Ion transport in yeast. Biochim. Biophys. Acta **650**:88–127.
3. **Carle, G. F., and M. V. Olson.** 1984. Separation of chromosomal DNA molecules from yeast by orthogonal-field-alternation gel electrophoresis. Nucleic Acids Res. **12**:5647–5664.
4. **Carle, G. F., and M. V. Olson.** 1985. An electrophoretic karyotype for yeast. Proc. Natl. Acad. Sci. USA **82**:3756–3760.
5. **Eisenberg, D.** 1984. Analysis of membrane and surface protein sequences with the hydrophobic moment plot. Annu. Rev. Biochem. **53**:595–623.
6. **Epstein, W., L. Wieczorek, A. Siebers, and A. Karlheinz.** 1984. Potassium transport in *Escherichia coli*: genetic and biochemical characterization of the K^+-transporting ATPase. Biochem. Soc. Trans. **12**:235–236.
7. **Goldin, S. M.** 1977. Active transport of sodium and potassium ions by the sodium and potassium ion-activated adenosine triphosphatase from renal medulla. J. Biol. Chem. **252**:5630–5642.
8. **Gustin, M. C., B. Martinac, Y. Saimi, M. R. Culbertson, and C. Kung.** 1986. Ion channels in yeast. Science **233**:1195–1197.
9. **Hesse, J. E., L. Weiczorek, K. Altendorf, A. S. Reicin, E. Dorus, and W. Epstein.** 1984. Sequence homology between two membrane transport ATPases, the Kdp-ATPase of *Escherichia coli* and the Ca^{2+}-ATPase of sarcoplasmic reticulum. Proc. Natl. Acad. Sci. USA **81**:4746–4750.
10. **Higgins, C. F., I. D. Hiles, G. P. C. Salmond, D. R. Gill, J. A. Downie, I. J. Evans, I. B. Holland, L. Gray, S. D. Buckel, A. W. Bell, and M. A. Hermodson.** 1986. A family of related ATP-binding subunits coupled to many distinct biological processes in bacteria. Nature (London) **323**:448–450.
11. **Holmes, D. S., and M. Quigley.** 1981. A rapid boiling method for the preparation of bacterial plasmids. Anal. Biochem. **114**:193–197.
12. **Ito, H., Y. Fukuda, K. Murata, and A. Kimura.** 1983. Transformation of intact yeast cells treated with alkali cations. J. Bacteriol. **153**:163–168.
13. **Kamb, A., L. E. Iverson, and M. A. Tanouye.** 1987. Molecular characterization of *Shaker*, a drosophila gene that encodes a potassium channel. Cell **50**:405–413.
14. **Kawakami, K., S. Noguchi, M. Noda, H. Takahashi, T. Ohta, M. Kawamura, H. Nojima, K. Nagano, T. Hirose, S. Inayama, H. Hayashida, M. Takashi, and S. Numa.** 1985. Primary structure of the Δ-subunit of *Torpedo californica* ($Na^+ + K^+$) ATPase deduced from cDNA sequence. Nature (London) **316**:733–736.
15. **Kyte, J., and R. F. Doolittle.** 1982. A simple method of displaying the hydropathic character of a protein. J. Mol. Biol. **157**:105–132.
16. **Laemmli, U. K.** 1970. Cleavage of structural proteins during the assembly of the head of bacteriophage T4. Nature (London) **227**:680–685.
17. **Lowry, O. H., N. J. Rosenbrough, A. L. Farr, and R. J. Randall.** 1951. Protein measurement with the Folin phenol reagent. J. Biol. Chem. **193**:265–275.
18. **Malpartida, F., and R. Serrano.** 1981. Proton translocation catalyzed by the purified yeast plasma membrane ATPase reconstituted in liposomes. FEBS Lett. **131**:351–354.
19. **Malpartida, F., and R. Serrano.** 1981. Reconstitution of the proton-translocating adenosine triphosphatase of yeast plasma membranes. J. Biol. Chem. **256**:4175–4177.
20. **Maniatis, T., E. F. Fritsch, and J. Sambrook.** 1982. Molecular cloning: a laboratory manual. Cold Spring Harbor Laboratory, Cold Spring Harbor, N.Y.
21. **Messing, J., R. Crea, and P. H. Seeburg.** 1981. A system for shotgun DNA sequencing. Nucleic Acids Res. **9**:309–321.
22. **Ohashi, A., J. Gibson, I. Gregor, and G. Schatz.** 1982. Import of proteins into mitochondria. J. Biol. Chem. **257**:13042–13047.
23. **Papazian, D. M., T. L. Schwarz, B. L. Tempel, Y. N. Jan, and L. Y. Jan.** 1987. Cloning of genomic and complementary DNA from *Shaker*, a putative potassium channel gene from *Drosophila*. Science **237**:749–753.
24. **Perkins, D.** 1949. Biochemical mutants in the smut fungus *Ustilago maydis*. Genetics **34**:607–626.
25. **Ramos, J., P. Contreras, and A. Rodriguez-Navarro.** 1985. A potassium transport mutant of *Saccharomyces cerevisiae*. Arch. Microbiol. **143**:88–93.
26. **Rodríguez-Navarro, A., M. R. Blatt, and C. L. Slayman.** 1986. A potassium-proton symport in *Neurospora crassa*. J. Gen. Physiol. **87**:649–674.
27. **Rodríguez-Navarro, A., and J. Ramos.** 1984. Dual system for potassium transport in *Saccharomyces cerevisiae*. J. Bacteriol. **159**:940–945.
28. **Sanger, F., S. Nicklen, and A. R. Coulson.** 1977. DNA sequencing with chain-terminating inhibitors. Proc. Natl. Acad. Sci. USA **74**:5463–5467.
29. **Serrano, R.** 1980. Effect of ATPase inhibitors on the proton pump of respiration deficient yeast. Eur. J. Biochem. **105**:419–424.
30. **Serrano, R.** 1984. Plasma membrane ATPase of fungi and plants as a novel type of proton pump. Curr. Top. Cell. Regul. **23**:87–126.
31. **Serrano, R., M. C. Kielland-Brandt, and G. R. Fink.** 1986. Yeast plasma membrane ATPase is essential for growth and has homology with ($Na^+ + K^+$), K^+- and Ca^{2+}-ATPases. Nature (London) **319**:689–693.
32. **Sherman, F., G. R. Fink, and C. Lawrence.** 1979. Methods in yeast genetics. Cold Spring Harbor Laboratory, Cold Spring Harbor, N.Y.
33. **Shull, G. E., L. K. Lane, and J. B. Lingrel.** 1986. Amino-acid sequence of the β-subunit of the ($Na^+ + K^+$)ATPase deduced from a cDNA. Nature (London) **321**:429–431.
34. **Shull, G. E., A. Schwartz, and J. B. Lingrel.** 1985. Amino-acid sequence of the catalytic subunit of the ($Na^+ + K^+$)ATPase deduced from a complementary DNA. Nature (London) **316**:691–695.
35. **Spindler, K. R., D. S. E. Rosser, and A. J. Berk.** 1984. Analysis of adenovirus transforming proteins from early regions 1A and 1B with antisera to inducible fusion antigens produced in *Escherichia coli*. J. Virol. **49**:132–141.
36. **Tempel, B. L., D. M. Papazian, T. L. Schwarz, Y. N. Jan, and L. Y. Jan.** 1987. Sequence of a probable potassium channel

component encoded at *shaker* locus of *Drosophila*. Science **237:** 770–775.

37. **Towbin, H., T. Staelin, and J. Gordon.** 1970. Electrophoretic transfer of proteins from polyacrylamide gels to nitrocellulose sheets: procedure and some applications. Proc. Natl. Acad. Sci. USA **79:**4350–4354.
38. **Walton, E. F., B. L. A. Carter, and J. R. Pringle.** 1979. An enrichment method for temperature-sensitive and auxotrophic mutants of yeast. Mol. Gen. Genet. **171:**111–114.
39. **Winston, J. F., F. Chumley, and G. R. Fink.** 1983. Eviction and transplacement of mutant genes in yeast. Methods Enzymol. **101:**211–228.